

# Highly Efficient and Reversible Absorption of SO<sub>2</sub> from Flue Gas Using Diamino Polycarboxylate Protic Ionic Liquid Aqueous Solutions

Haiming Zhang,<sup>†</sup> Bin Jiang, Na Yang,<sup>†</sup> Na Zhang, Luhong Zhang,<sup>‡</sup> Zhaohe Huang, Xiaoming Xiao, and Xiaowei Tantai<sup>\*‡</sup>

School of Chemical Engineering and Technology, Tianjin University, Tianjin 300072, People's Republic of China

## Supporting Information

**ABSTRACT:** Ionic liquid (IL) aqueous solutions (aq) have emerged as promising candidates for SO<sub>2</sub> absorption. In this work, a new series of diamino polycarboxylate protic ionic liquids (DPPILs) aq with low viscosities and high stabilities were developed and used for SO<sub>2</sub> capture. All of the prepared absorbents could efficiently absorb low-concentration SO<sub>2</sub> in simulated flue gas. Among them, DPPILs aq based on citric acid (CA) presented the most excellent SO<sub>2</sub> desorption performance; nearly all absorbed SO<sub>2</sub> could be easily desorbed under mild conditions. Particularly, *N,N*-dimethylethylenediamine citrate [DMEDA][CA] showed the highest available absorption capacity toward 0.2 vol % SO<sub>2</sub> (up to 0.51 mol<sub>SO<sub>2</sub></sub>/mol<sub>ILs</sub> and 0.058 g<sub>SO<sub>2</sub></sub>/g<sub>abs</sub> in 50 wt % aq at 20 °C), which also presented satisfactory SO<sub>2</sub>/CO<sub>2</sub> selectivity, reusability, and SO<sub>2</sub> removal efficiency. Fourier transform infrared and nuclear magnetic resonance spectroscopic analyses revealed that the protonation of [DMEDA]<sup>+</sup> and [CA]<sup>-</sup> promoted SO<sub>2</sub> absorption. Overall, the studied DPPILs aq with excellent physical properties, SO<sub>2</sub> absorption–desorption performance, and stability may have a great perspective in industrial SO<sub>2</sub> removal.

## 1. INTRODUCTION

Excessive sulfur dioxide (SO<sub>2</sub>) in the atmosphere will create adverse effects on the environment and human health.<sup>1</sup> Currently, the flue gas desulfurization (FGD) process is deemed to be the most effective measure to control the atmospheric SO<sub>2</sub> concentration. Among commercially available processes, the limestone–gypsum method is the most widely used technique.<sup>2</sup> However, the shortcomings of this process are obvious, such as the non-renewability of absorbents and the production of waste effluents and solid byproduct (CaSO<sub>4</sub>). Another widely used process is the ammonia scrubbing technique.<sup>3</sup> Nevertheless, the volatilization of the absorption agent is inevitable, which could cause secondary pollution to the environment, and the regeneration of absorbents is a high-energy-consumption process. Consequently, it is still highly desired to develop novel renewable, stable, and energy-saving absorbents for the FGD process.

Over the past few decades, ionic liquids (ILs) have been proposed as attractive candidates for acid gas capture as a result of their unique properties, such as high thermal stability, negligible vapor pressure, and tunable structure.<sup>4–9</sup> Han et al. first reported that tetramethylguanidinium lactate [TMG][L] could capture SO<sub>2</sub> with absorption capacity up to 0.978 mol<sub>SO<sub>2</sub></sub>/mol<sub>ILs</sub> at 40 °C and 8% SO<sub>2</sub> in 2004.<sup>10</sup> Subsequently, numerous ILs have been explored for SO<sub>2</sub> absorption, including guanidinium-derived,<sup>11,12</sup> imidazolium-derived,<sup>13–15</sup> hydroxyl-ammonium-derived,<sup>16,17</sup> and ether-functionalized ILs.<sup>18,19</sup> Although these ILs exhibited high SO<sub>2</sub> loading capacities (especially functional ILs), the ultrahigh viscosities and costs hampered their large-scale application.

To overcome the drawbacks of ILs mentioned above, a feasible and promising strategy is to develop IL aqueous solutions (aq) by mixing low-cost ILs with water. Huang et al. reported that the aq of hydroxylammonium dicarboxylate ILs could absorb SO<sub>2</sub> efficiently and the mixed absorbents showed low viscosities and satisfactory mass transfer performance.<sup>20</sup> Wu et al. developed a series of aqueous triethylenetetramine tetralactate [TETA][L] solutions for SO<sub>2</sub> absorption.<sup>21</sup> It was found that the absorption–desorption properties of SO<sub>2</sub> in ILs aq could be easily tuned by varying the compositions of ILs. In our previous work, a novel triamine-based IL aq was used for SO<sub>2</sub> capture, and the results showed that the excellent SO<sub>2</sub> absorption capacity, especially at very low partial pressures, was contributed to the chemical absorption originating from the pH-buffering effect.<sup>22</sup> Obviously, all of these benign absorbents were composed of protic ionic liquid (PILs), which could be easily synthesized by low-cost materials through direct acid–base neutralization in contrast to aprotic ionic liquids (APIs).<sup>23,24</sup> The capture of SO<sub>2</sub> using PILs aq is based on a buffer mechanism.<sup>25,26</sup> First, SO<sub>2</sub> dissolves in aq and undergoes hydration to form H<sub>2</sub>SO<sub>3</sub>. Subsequently, H<sub>2</sub>SO<sub>3</sub> ionizes into H<sup>+</sup>, HSO<sub>3</sub><sup>-</sup>, and SO<sub>3</sub><sup>2-</sup>. These processes could be promoted taking advantages of the protonation of free carboxylate anions (–COO<sup>-</sup>) or amines in aq. Therefore, PILs aq used for efficient SO<sub>2</sub> absorption (especially for the flue gas with a low SO<sub>2</sub> concentration) should meet at least one of the following requirements: (1) the acids selected for synthesizing ILs should be weaker than H<sub>2</sub>SO<sub>3</sub>, implying that

Received: May 29, 2019

Revised: August 2, 2019

Published: August 12, 2019

the  $pK_a$  values of the acids should be higher than 1.8, and (2) the basicities of amines should be strong enough.<sup>27–29</sup> Of note, if the acidities of the selected acids are too weak or the basicities of amines are too strong, it tends to cause irreversible absorption and enormous energy demand for absorbent regeneration. In addition, because  $SO_2$  desorption is usually carried out at a high temperature, the thermostabilities and volatilities of PILs and the derived acids should also be well-considered.

Lately, diamino protic ionic liquids (DPILs) have attracted intensive attention owing to their exceptional characteristics, such as the higher stability and moderate alkalinity compared to traditional PILs.<sup>30,31</sup> Generally, DPILs were obtained by neutralizing organic bases containing both primary and tertiary amines with carboxylic acids.<sup>32,33</sup> DPILs with facilely tunable alkalinity through subtle combination bases and acids have been widely studied for  $CO_2$  capture. These DPILs were found to readily achieve high  $CO_2$  loading capacities and low absorption enthalpies, which indicated that DPILs are a promising candidate for acid gas capture with high capacity and energy savings.<sup>34,35</sup> Herein, we develop a series of diamino polycarboxylate protic ionic liquids (DPPILs) aq for  $SO_2$  capture. To the best of our knowledge, DPPILs have not been synthesized and used for  $SO_2$  absorption thus far. The corresponding DPPILs could be easily synthesized by neutralizing *N,N*-dimethylethylenediamine (DMEDA) and (3-dimethylamino)-1-propylamine (DMAPA) with succinic acid (SUC), tartaric acid (TA), and citric acid (CA) (see Scheme 1 for structures of amines and acids). DMEDA and

non-volatile poly(carboxylic acid)s. According to previous reports, polycarboxylate-based ILs tended to exhibit more excellent  $SO_2$  absorption–desorption properties than monocarboxylate-based ILs.<sup>20,36,37</sup> In this work, the physical properties of the prepared absorbents were studied comprehensively. The influences of DPPIL structures, DPPIL concentrations, absorption temperature, and  $SO_2$  concentration on the absorption performance were systematically investigated. The desulfurization performance of the studied absorbent on simulated flue gas was also evaluated. Moreover, the absorption mechanism was clarified by Fourier transform infrared spectroscopy (FTIR) and proton nuclear magnetic resonance ( $^1H$  NMR).

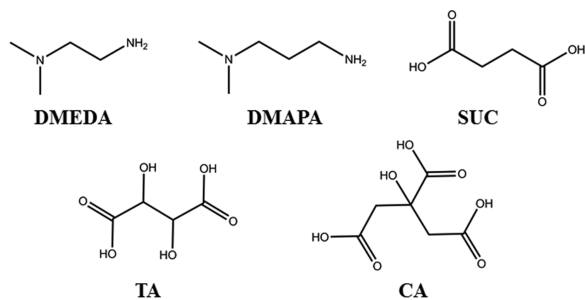
## 2. EXPERIMENTAL SECTION

**2.1. Materials.** DMEDA ( $\geq 99\%$ ) and DMAPA ( $\geq 99\%$ ) were purchased from Aladdin Industrial Corporation. SUC ( $\geq 99.5\%$ ), TA ( $\geq 99.5\%$ ), and CA ( $\geq 99.5\%$ ) were provided by Tianjin Chemart Chemical Technology Co., Ltd.  $SO_2$  (99.9%) and  $N_2$  (99.99%) were supplied by Tianjin Dongxiang Specialty Gases Co., Ltd. All chemicals were used without further purification.

**2.2. Preparation of  $SO_2$  Absorbents.** All DPPILs used in this work were synthesized by neutralizing equimolar diamines with poly(carboxylic acid)s referring to reports (the actual quantities of the starting materials are shown in Table S1 of the Supporting Information).<sup>7,17</sup> For instance, the preparation process of [DMEDA]-[CA] is as follows: 0.1 mol of DMEDA was dissolved in 50 mL of deionized water and loaded into a 250 mL flask, which was equipped with a reflux condenser and placed in an ice–water bath. Subsequently, 0.1 mol of CA dissolved in 50 mL of deionized water was added dropwise into the flask within 1 h under vigorous stirring. The reaction was stirred for 24 h at room temperature. Water was removed by rotary evaporation, and the water contents of the obtained DPPILs were determined below 1 wt % (Table S2 of the Supporting Information). Of note, the equivalence point pH values (Table S3 of the Supporting Information) of each neutralization reaction were determined by the titration method (0.1 mol/L aq), which were very close to those of 0.1 mol/L DPPILs aq (Table S3 of the Supporting Information), thus proving that the obtained stoichiometric ratios were the expected 1:1. Additionally, the corresponding DPPILs aq were obtained by mixing DPPILs with water at the certain mass ratios, as shown in Table 1.

**2.3. Characterization.** The  $^1H$  NMR spectra of DPPILs were recorded on a 500 MHz spectrometer (Bruke Avance III, Germany), and the characterization results are shown in the Supporting Information, which presented that both primary and tertiary amines of DMEDA and DMAPA were protonated in neat DPPILs. It could be found that there were no obvious signals of neutral acids and bases in  $^1H$  NMR spectra. Therefore, although there may be neutral bases and acids in DPPILs, their contents could be neglected and the protons from acids could be considered to be completely transferred

**Scheme 1. Structures of Amines and Acids Used To Synthesize DPPILs**



DMAPA are the most common organic bases for DPIL synthesis, with the advantages of small molecular weight and moderate basicities. SUC, TA, and CA are all inexpensive and

**Table 1. Physical Properties (25 °C) of the Prepared  $SO_2$  Absorbents**

absorbent	water content (wt %)	density (g/mL)		viscosity (cP)	
		before absorption	after absorption	before absorption	after absorption
[DMEDA][SUC], 50 wt %	49.33	1.1623	1.1609	1.69	2.74
[DMEDA][TA], 50 wt %	50.41	1.1756	1.1734	1.97	3.03
[DMEDA][CA], 60 wt %	41.03	1.2163	1.2144	4.83	6.86
[DMEDA][CA], 50 wt %	50.63	1.1963	1.1955	2.33	4.41
[DMEDA][CA], 40 wt %	59.11	1.1722	1.1707	1.73	3.79
[DMEDA][CA], 30 wt %	69.29	1.1578	1.1566	1.44	2.47
[DMEDA][CA], 20 wt %	80.32	1.1530	1.1522	1.13	1.90
[DMAPA][SUC], 50 wt %	50.33	1.1732	1.1718	1.94	3.14
[DMAPA][TA], 50 wt %	49.86	1.1865	1.1844	2.17	3.31
[DMAPA][CA], 50 wt %	50.31	1.2102	1.2094	2.92	4.31

to amines. Additionally, electrospray ionization mass spectrometry (ESI-MS, Agilent 1100 LC/DAD/MSD) was used to characterize the anions and cations in 50 wt % DPPILs aq. The results (Supporting Information) showed that the tertiary amines of DMEDA and DMAPA were not protonated completely in 50 wt % DPPILs aq, and the stable anions and cations were  $[\text{SUC}]^-$ ,  $[\text{TA}]^-$ ,  $[\text{CA}]^-$ ,  $[\text{DMEDAH}]^+$ , and  $[\text{DMAPA}]^+$ . The densities of unreacted and 0.2 vol %  $\text{SO}_2$  saturated (25 °C) absorbents were measured using a precalibrated (deionized water) 5 mL pycnometer. Each sample was determined 5 times to report the average, and the uncertainty was estimated to be less than  $\pm 1\%$ . The viscosities of DPPILs aq before and after  $\text{SO}_2$  absorption (0.2 vol %  $\text{SO}_2$  and 25 °C) were measured by a viscometer (Brookfield DV-II+ Pro). Standard silicone oil was used to calibrate the viscometer. Each measure was repeated 5 times to obtain an average, and the uncertainty was estimated to be  $\pm 2.5\%$ . The thermostability of DPPILs was evaluated by thermogravimetric analysis (TGA) and derivative thermogravimetry (DTG) (NETZSCH). Furthermore, the absorption mechanism was clarified through FTIR (Bruker, TENSOR II, Germany) and  $^1\text{H}$  NMR (500 MHz, Bruke Avance III, Germany) spectroscopies.

**2.4. Absorption and Desorption of  $\text{SO}_2$ .** The absorption and desorption experiments were carried out using the previously reported method.<sup>28,29,38</sup> The experimental system is shown in Figure 1. To

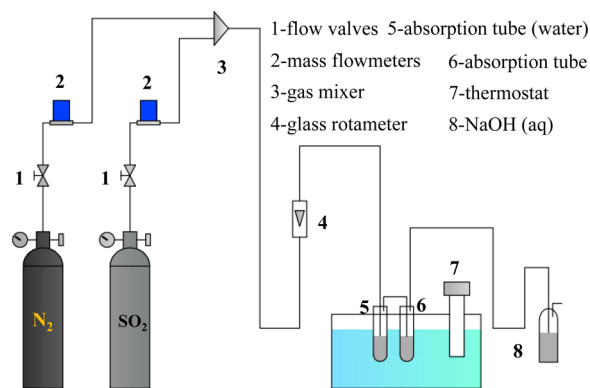


**Figure 1.** Schematic diagram of the absorption–desorption experimental system.

validate the feasibility of the absorption–desorption experimental system, the water loss ratios in the absorption tube (water), the outlet  $\text{SO}_2$  concentrations of the absorption tube (water), and the water content variations of the absorbents during  $\text{SO}_2$  absorption–desorption were determined and the results are summarized in Tables S4–S6 of the Supporting Information. In a typical absorption process, simulated flue gas (0.2 vol %  $\text{SO}_2$  and 99.8 vol %  $\text{N}_2$ ) at 100 mL/min was successively bubbled through two glass tubes loading about 2 g of deionized water (to offset the water evaporated) and DPPILs aq, respectively. The glass tubes were partly immersed in a thermostatic water bath with the desired temperature. The gas flow rates were controlled by mass flowmeters. The amount of absorbed  $\text{SO}_2$  was measured using the iodine titration method (HJ/T 56-2000, a standard method of the State Environmental Protection Administration of China). For absorption under different  $\text{SO}_2$  concentrations, the certain inlet  $\text{SO}_2$  concentration was controlled by tuning the flow rate ratio of  $\text{SO}_2$  and  $\text{N}_2$ . The desorption procedure was similar to that described above, only the simulated flue gas (100 mL/min) was replaced by pure  $\text{N}_2$  (50 mL/min) and the desorption efficiency (DE) was calculated by the following equation:

$$DE = (R_a - R_d)/R_a \times 100\% \quad (1)$$

where  $R_a$  is the saturated molar  $\text{SO}_2$  absorption capacity and  $R_d$  is the desorption residue. All measurements were repeated 3 times to obtain the averages, and it was estimated that the uncertainty of the results was less than  $\pm 5\%$ . To evaluate the desulfurization performance of the studied  $\text{SO}_2$  absorbent, the inlet and outlet  $\text{SO}_2$  concentrations were

determined by a gas analyzer (Testo 350) and the  $\text{SO}_2$  removal efficiency (RE) was calculated by the following formula:

$$RE = (C_{in} - C_{out})/C_{in} \times 100\% \quad (2)$$

where  $C_{in}$  and  $C_{out}$  were the  $\text{SO}_2$  concentrations in the inlet and outlet, respectively.

### 3. RESULTS AND DISCUSSION

**3.1. Physical Properties of  $\text{SO}_2$  Absorbents.** The densities and viscosities of unreacted and 0.2 vol %  $\text{SO}_2$  saturated DPPILs aq were determined at 25 °C. As shown in Table 1, the densities of the prepared absorbents increased with the increase of the molecular weight of DPPILs and the concentration of DPPILs in the mixed absorbents. The viscosity showed the same trend as the density. Additionally, it could be found that there were no significant differences in the densities and viscosities of these absorbents before and after  $\text{SO}_2$  absorption. Of note, all absorbents prepared in this work presented extremely low viscosities (like water), whereas the viscosities of neat ILs were usually higher than 300 cP,<sup>20</sup> indicating that the viscosities of IL absorbents could be significantly reduced by mixing with water, and it could be inferred that the prepared absorbents with low viscosities could be potentially applied for the FGD process.

**3.2. Absorption–Desorption of  $\text{SO}_2$ .** **3.2.1. Absorption Mechanism.** In this work, FTIR and  $^1\text{H}$  NMR were used to clarify the absorption mechanism of  $\text{SO}_2$  in 50 wt % [DMEDA][CA] aq. The FTIR spectra before and after  $\text{SO}_2$  absorption are shown in Figure 2. In comparison to the FTIR

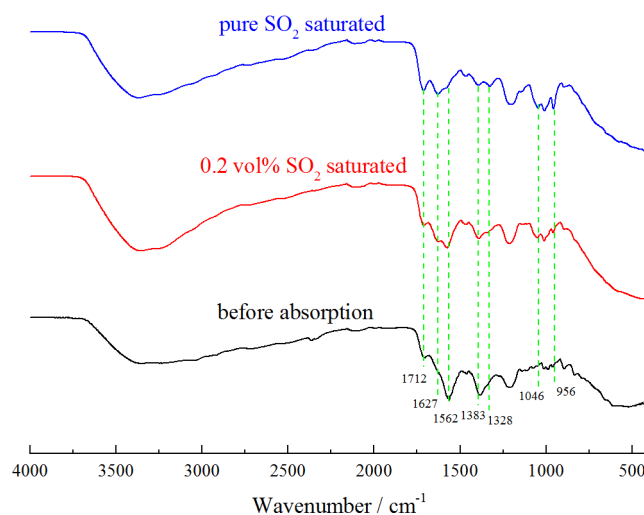
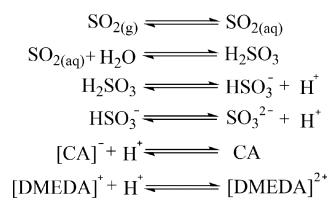


**Figure 2.** FTIR spectra of 50 wt % [DMEDA][CA] aq before and after absorption of  $\text{SO}_2$ .

spectrum of the virgin absorbent, three characteristic peaks of absorbed  $\text{SO}_2$  appeared after absorption. The new peak centered at  $956\text{ cm}^{-1}$  could be attributed to the stretching vibration of S–O bonds in  $\text{SO}_3^{2-}$  or  $\text{HSO}_3^-$ , which indicated that the studied absorbent could capture  $\text{SO}_2$  via chemical interaction.<sup>22,39</sup> The new peak at  $1046\text{ cm}^{-1}$  could be assigned to the S=O stretching vibration of  $\text{SO}_2$ ,  $\text{H}_2\text{SO}_3$ ,  $\text{HSO}_3^-$ , or  $\text{SO}_3^{2-}$ .<sup>40,41</sup> The characteristic peak presented at  $1328\text{ cm}^{-1}$  was ascribed to the asymmetry stretching vibration of dissolved  $\text{SO}_2$ .<sup>42,43</sup> Additionally, it was clear that captured  $\text{SO}_2$  presented a significant effect on –COOH and –COO<sup>–</sup> in aq. More concretely, the symmetric ( $1562\text{ cm}^{-1}$ ) and asymmetric ( $1383$

$\text{cm}^{-1}$ ) vibrations of  $-\text{COO}^-$  were weakened gradually during  $\text{SO}_2$  absorption, whereas the vibrations ( $1712$  and  $1627$   $\text{cm}^{-1}$ ) associated with  $-\text{COOH}$  were enhanced notably, implying that  $-\text{COOH}$  was formed during the absorption process.<sup>28,29,44</sup> Meanwhile, in comparison to the  $^1\text{H}$  NMR spectrum (Figure S1 of the Supporting Information) of the virgin absorbent, the spectrum of the  $0.2$  vol %  $\text{SO}_2$  saturated absorbent presented a new peak at  $9.97$  ppm, which could be assigned to the H atom bonded to the N atom of  $[\text{DMEDA}]^+$ ,<sup>45,46</sup> demonstrating that  $[\text{DMEDA}]^+$  also played an important role in  $\text{SO}_2$  capture. Therefore, on the basis of the above analysis and previous reports, a plausible  $\text{SO}_2$  absorption mechanism was illustrated in Scheme 2.

### Scheme 2. $\text{SO}_2$ Absorption Mechanism in 50 wt % $[\text{DMEDA}][\text{CA}]$ aq



**3.2.2. Effect of Different DPPILs on  $\text{SO}_2$  Absorption–Desorption.** It was found that neat  $[\text{DMEDA}][\text{TA}]$  and  $[\text{DMAPA}][\text{TA}]$  were in a solid state within the range of  $20$ – $60$   $^\circ\text{C}$ . Besides, for  $[\text{DMEDA}][\text{SUC}]$ ,  $[\text{DMEDA}][\text{CA}]$ ,  $[\text{DMAPA}][\text{SUC}]$ , and  $[\text{DMAPA}][\text{CA}]$ , although they could flow at  $40$   $^\circ\text{C}$  (gel at  $20$   $^\circ\text{C}$ ), their viscosities increased rapidly and turned into gel in the process of absorption at  $40$   $^\circ\text{C}$ . Thus, only the absorption–desorption properties of DPPILs aq were discussed in the following sections. To investigate the influence of different DPPILs on  $\text{SO}_2$  absorption–desorption properties, the absorption–desorption experiments were carried out at  $20$   $^\circ\text{C}$ ,  $1$  atm, and simulated flue gas ( $0.2$  vol %  $\text{SO}_2$  and  $99.8$  vol %  $\text{N}_2$ ) at  $100$  mL/min and  $80$   $^\circ\text{C}$ ,  $1$  atm, and pure  $\text{N}_2$  at  $50$  mL/min, respectively. For all 50 wt % DPPILs aq prepared in this work, the  $\text{SO}_2$  absorption and desorption equilibriums could be achieved within  $120$  and  $60$  min as shown in Figures S2 and S3 of the Supporting Information, respectively, indicating that the prepared absorbents presented excellent mass transfer performance. The  $\text{SO}_2$  absorption capacities (Table S7 of the Supporting Information) and desorption residues are shown in Figure 3. Obviously, all 50 wt % DPPILs aq could efficiently capture low-concentration  $\text{SO}_2$ . The  $\text{SO}_2$  loading capacities were up to  $0.67$ ,  $0.61$ ,  $0.53$ ,  $0.73$ ,  $0.67$ , and  $0.54$   $\text{mol}_{\text{SO}_2}/\text{mol}_{\text{ILs}}$  for  $[\text{DMEDA}][\text{SUC}]$ ,  $[\text{DMEDA}][\text{TA}]$ ,  $[\text{DMEDA}][\text{CA}]$ ,  $[\text{DMAPA}][\text{SUC}]$ ,  $[\text{DMAPA}][\text{TA}]$ , and  $[\text{DMAPA}][\text{CA}]$ , respectively. It could be found that the  $\text{SO}_2$  absorption capacities of DPPILs were closely related to the  $\text{p}K_a$  values (Table S8 of the Supporting Information) of diamines and poly(carboxylic acid)s selected for synthesizing ILs. The higher the  $\text{p}K_a$  values of the amines and acids, the higher the absorption capacities could be achieved. The  $\text{SO}_2$  desorption residue showed the same trend as the absorption capacity. Of note, the  $\text{SO}_2$  desorption efficiencies in 50 wt %  $[\text{DMEDA}][\text{CA}]$  and  $[\text{DMAPA}][\text{CA}]$  aq were up to  $97$  and  $93\%$  within  $1$  h, respectively, far higher than those of other DPPIL absorbents. The pH values of 50 wt %  $[\text{DMEDA}][\text{CA}]$  and  $[\text{DMAPA}][\text{CA}]$  aq were  $4.68$  and  $5.17$  at  $25$   $^\circ\text{C}$ , respectively,

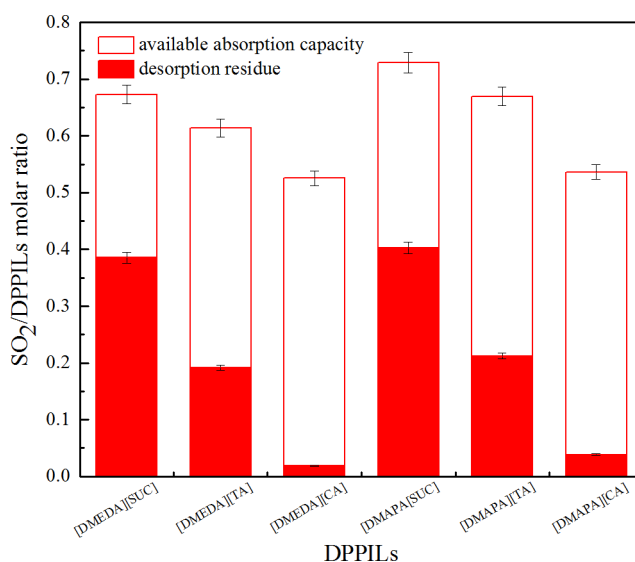


**Figure 3.**  $\text{SO}_2$  absorption capacities and desorption residues of different DPPILs (aq, 50 wt %).

within the appropriate pH range ( $4.5$ – $5.5$ ) for the highly efficient and reversible  $\text{SO}_2$  capture proposed by Huang et al.<sup>20</sup> The available absorption capacities of 50 wt %  $[\text{DMEDA}][\text{SUC}]$ ,  $[\text{DMEDA}][\text{TA}]$ ,  $[\text{DMEDA}][\text{CA}]$ ,  $[\text{DMAPA}][\text{SUC}]$ ,  $[\text{DMAPA}][\text{TA}]$ , and  $[\text{DMAPA}][\text{CA}]$  aq were also calculated, with the values of  $0.29$ ,  $0.42$ ,  $0.51$ ,  $0.33$ ,  $0.46$ , and  $0.49$   $\text{mol}_{\text{SO}_2}/\text{mol}_{\text{ILs}}$ , corresponding to  $0.045$ ,  $0.057$ ,  $0.058$ ,  $0.047$ ,  $0.058$ , and  $0.053$   $\text{g}_{\text{SO}_2}/\text{g}_{\text{abs}}$ , respectively. Thus, considering the higher available capacity,  $[\text{DMEDA}][\text{CA}]$  was selected for subsequent studies.

**3.2.3. Effect of the DPPIL Concentration on  $\text{SO}_2$  Absorption–Desorption.** The influence of the DPPIL concentration on  $\text{SO}_2$  absorption–desorption was also investigated. As shown in Figure 4, the molar  $\text{SO}_2$  absorption capacity of  $[\text{DMEDA}][\text{CA}]$  increased with the decrease of the DPPIL concentration and the increase of the water content of

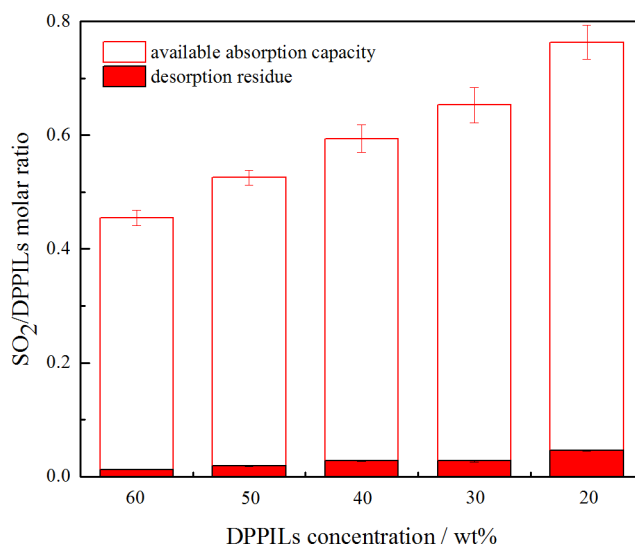


**Figure 4.** Molar  $\text{SO}_2$  absorption capacities and desorption residues of  $[\text{DMEDA}][\text{CA}]$  aq with different concentrations at  $20$   $^\circ\text{C}$  and  $0.2$  vol %  $\text{SO}_2$ .

the absorbent. For instance, the  $\text{SO}_2$  loading capacity of [DMEDA][CA] increased from 0.46 to 0.76  $\text{mol}_{\text{SO}_2}/\text{mol}_{\text{ILs}}$  as the DPPIL concentration decreased from 60 to 20 wt %. The solubility of 0.2 vol %  $\text{SO}_2$  in deionized water was also measured at 20 °C, with the value of 0.0007  $\text{mol}_{\text{SO}_2}/\text{mol}_{\text{H}_2\text{O}}$  (0.0025  $\text{g}_{\text{SO}_2}/\text{g}_{\text{H}_2\text{O}}$ ), which was negligible compared to those of the studied absorbents, indicating that DPPILs played the major role in  $\text{SO}_2$  capture rather than water. Additionally, it could be found that the desorption residue also increased slightly with the decrease of the DPPIL concentration. Perhaps this was because, although the overall dissolution behavior of  $\text{SO}_2$  in DPPILs aq cannot be described by Henry's law, the transfer of  $\text{SO}_2$  molecules from flue gas to absorbent (converting to  $\text{SO}_{2(\text{aq})}$ ) could still be expressed by that. Thus, the  $\text{SO}_{2(\text{aq})}$  concentration in the absorbent could be considered as a constant value, whereas the concentrations of  $\text{HSO}_3^-$  and  $\text{SO}_3^{2-}$  decreased with the increase of the water content, resulting in the enhanced hydration of  $\text{SO}_2$  and ionization of  $\text{H}_2\text{SO}_3$  according to Le Chatelier's principle.<sup>21</sup> Furthermore, as shown in Figure 5, the gravimetric available

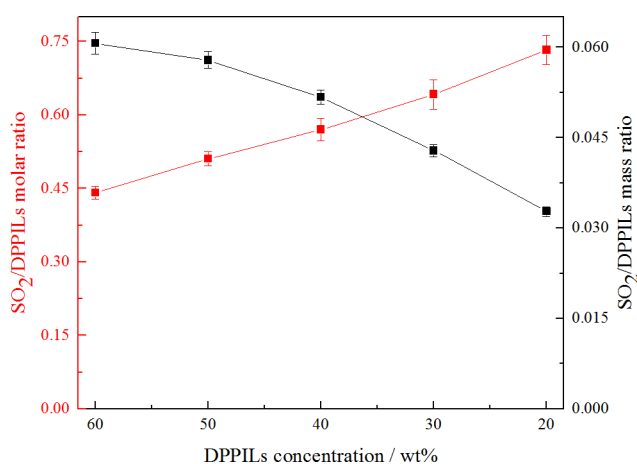


**Figure 5.** Available  $\text{SO}_2$  capacities in [DMEDA][CA] aq with different DPPIL concentrations at 20 °C and 0.2 vol %  $\text{SO}_2$ .

capacities of [DMEDA][CA] aq decreased from 0.061 to 0.033  $\text{g}_{\text{SO}_2}/\text{g}_{\text{abs}}$  as the DPPIL content decreased from 60 to 20 wt %, showing a contrary trend to the molar available  $\text{SO}_2$  capacities. Of note, although a high concentration of DPPILs was beneficial to mass absorption capacity of  $\text{SO}_2$ , it could lead to an increase in cost and viscosity of the absorbent (more than 300 cP for 10 wt % [DMEDA][CA] aq); thus, 50 wt % [DMEDA][CA] aq was still used in subsequent investigations.

**3.2.4. Effect of the Temperature on  $\text{SO}_2$  Absorption.** The temperature dependence of the  $\text{SO}_2$  absorption by 50 wt % [DMEDA][CA] aq at 1 atm with 0.2 vol %  $\text{SO}_2$  was investigated. It can be seen from Figure 6 that the  $\text{SO}_2$  loading capacity significantly decreased with the increase of the temperature, which was consistent with previous reports.<sup>47–49</sup> For instance, the saturated  $\text{SO}_2$  absorption capacity in 50 wt % [DMEDA][CA] aq was up to 0.53  $\text{mol}_{\text{SO}_2}/\text{mol}_{\text{ILs}}$  at 20 °C, while it decreased to 0.18  $\text{mol}_{\text{SO}_2}/\text{mol}_{\text{ILs}}$  at 60 °C. The results verified that absorbed  $\text{SO}_2$  could be released and the absorbent can be easily regenerated by heat treatment.

**3.2.5. Effect of the  $\text{SO}_2$  Concentration on Absorption.** The effect of the  $\text{SO}_2$  concentration in simulated flue gas on the

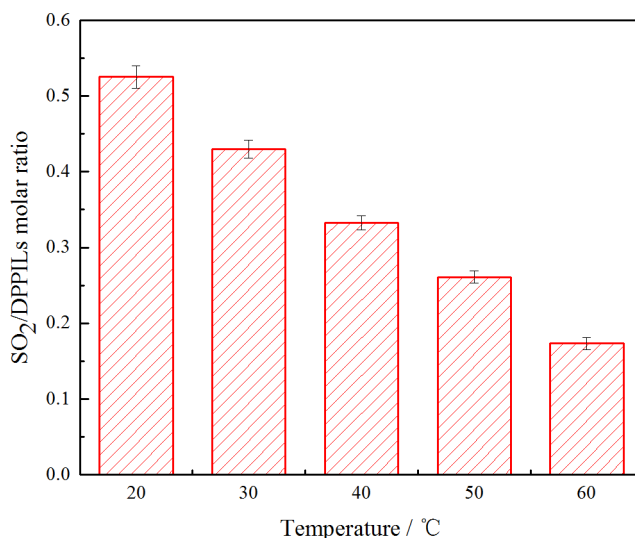


**Figure 6.** Effect of the temperature on  $\text{SO}_2$  absorption in 50 wt % [DMEDA][CA] aq at 1 atm with 0.2 vol %  $\text{SO}_2$ .

absorption capacity was investigated at 40 °C. As depicted in Figure 7, the  $\text{SO}_2$  absorption capacity elevated gradually with

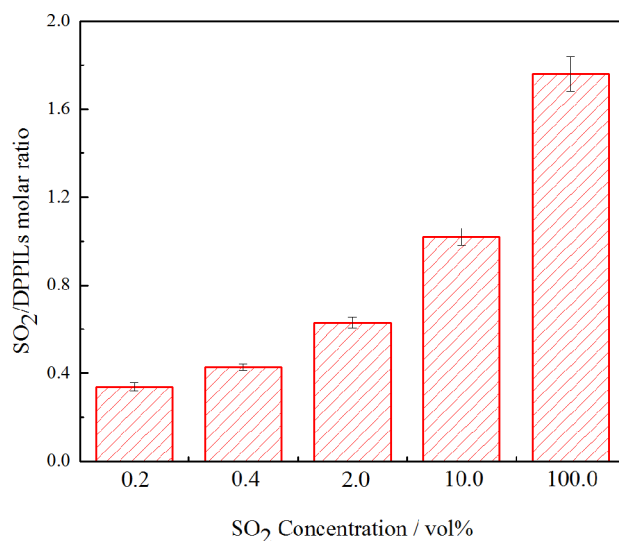


**Figure 7.** Effect of the  $\text{SO}_2$  concentration on absorption in 50 wt % [DMEDA][CA] aq at 40 °C.

the increase of the  $\text{SO}_2$  concentration in simulated flue gas. More specifically, the  $\text{SO}_2$  absorption capacity of 50 wt % [DMEDA][CA] (aq) increased from 0.34 to 1.76  $\text{mol}_{\text{SO}_2}/\text{mol}_{\text{ILs}}$  as the  $\text{SO}_2$  concentration increased from 0.2 to 100 vol % at 40 °C. The results implied that the  $\text{SO}_2$ -saturated absorbent could be easily regenerated by reducing the  $\text{SO}_2$  concentration. Additionally, it was clear that the  $\text{SO}_2$  loading capacity increased more remarkably in the low  $\text{SO}_2$  concentration range than in the high  $\text{SO}_2$  concentration range, indicating that the studied absorbent may interact with  $\text{SO}_2$  via chemical interaction according to previous reports.<sup>20,22</sup>

The absorption capacity of pure  $\text{CO}_2$  in 50 wt % [DMEDA][CA] aq was also determined, with the value of 0.10  $\text{mol}_{\text{CO}_2}/\text{mol}_{\text{ILs}}$  (0.008  $\text{g}_{\text{CO}_2}/\text{g}_{\text{abs}}$ ) at 40 °C and 1 atm. It was calculated that the gravimetric absorption capacity of pure  $\text{SO}_2$  in 50 wt % [DMEDA][CA] aq was 25 times higher than

Table 2. Comparison to Other IL Aqueous Solutions

absorbent	absorption ( $T_a$ , °C; SO <sub>2</sub> , vol %)	SO <sub>2</sub> capacity		desorption ( $T_d$ , °C; N <sub>2</sub> , mL/min; $t$ , min)	DE (%)	reference
		mol/mol <sup>a</sup>	g/g <sup>b</sup>			
[DMEDA][CA], 50 wt %	(40, 0.2)	0.34	0.039	(80, 50, 60)	97	this work
	(40, 0.4)	0.43	0.050			
[DMEA][glutamate], 60 wt %	(40, 0.4)	0.36	0.058	(100, 70, 60)	84	20
[TETA]L <sub>4</sub> , 70 wt %	(60, 3)	1.22	0.145	(100, 50, 300)	96	21
[PEDETAH][SO <sub>4</sub> ] <sub>0.5</sub> , 30 wt %	(40, 0.4)	0.68	0.044	(110, –, 60)	95 <sup>c</sup>	22
[BTMEDA]Cl, 23 wt %	(30, 100)	1.53	0.102	(60, 20, 60)	34	27

<sup>a</sup>mol<sub>SO<sub>2</sub></sub>/mol<sub>IL</sub>, <sup>b</sup>g<sub>SO<sub>2</sub></sub>/g<sub>abs</sub>. <sup>c</sup>DE with pure SO<sub>2</sub>-saturated absorption capacity as a reference.

that of CO<sub>2</sub>, indicating that the studied absorbent exhibited considerable SO<sub>2</sub>/CO<sub>2</sub> selectivity. Of note, the absorption capacity of 0.2 vol % SO<sub>2</sub> was still 4.8 times higher than that of pure CO<sub>2</sub>, and the concentration of CO<sub>2</sub> in flue gas was usually within the range of 10–15% in practice, implying that the studied absorbent could be employed as the selective absorbent for SO<sub>2</sub> absorption.

For comparison, the SO<sub>2</sub> absorption–desorption properties of the studied absorbent and the previously reported ILs aq are shown in Table 2. The results presented that the studied absorbent exhibited competitive SO<sub>2</sub> solubility at low SO<sub>2</sub> partial pressure. Meanwhile, nearly all SO<sub>2</sub> captured by the studied absorbent could be easily desorbed under mild conditions, showing more excellent desorption efficiency than others, which implied that the studied absorbent could be used as the low-energy-consumption absorbent for the FGD process. Therefore, comprehensively considering the excellent absorption–desorption properties, simple synthesis process, and relatively low cost, it could be expected that the studied absorbent held the potential for industrial application.

**3.2.6. Stability and Reusability of the SO<sub>2</sub> Absorbent.** The stability and reusability of the absorbent are important for evaluating its industrial application prospects. In this work, the thermostability of neat [DMEDA][CA] was explored. As shown in Figure 8, the decomposition temperature (5% weight loss) of [DMEDA][CA] was up to 175 °C, far above the desorption temperature commonly used in practice (100–120 °C for amine methods), indicating that the studied absorbent was stable enough during the absorption–desorption process. To investigate the long-time stability of 50 wt % [DMEDA][CA] aq, the studied absorbent was first saturated with 0.2 vol

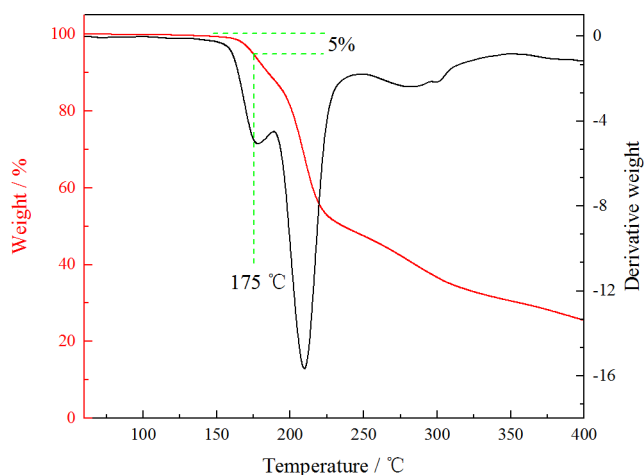


Figure 8. TGA and DTG curves of [DMEDA][CA].

% SO<sub>2</sub> and kept for 12 h at 40 °C and then absorbed SO<sub>2</sub> was desorbed by bubbling N<sub>2</sub> and kept for another 12 h at 80 °C. The procedure was repeated for 10 consecutive days, and the stability was evaluated by <sup>1</sup>H NMR (Figure 9). Clearly, in

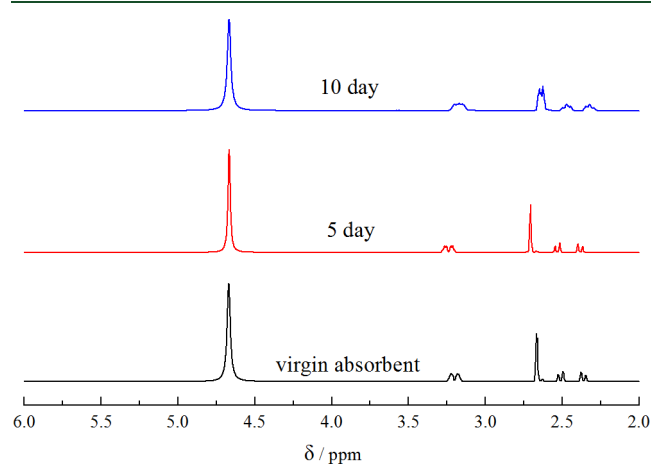


Figure 9. <sup>1</sup>H NMR spectra (DMSO-*d*<sub>6</sub>) of 50 wt % [DMEDA][CA] aq for different days of reuse.

comparison to the spectrum of the virgin absorbent, there was no obvious difference in the spectra of the absorbent used for a long time, indicating that the studied absorbent could be stable for a long time. Additionally, the reusability of 50 wt % [DMEDA][CA] aq was also investigated, and the absorption–desorption experiments were conducted at 40 °C, 1 atm, and pure SO<sub>2</sub> at 50 mL/min and 80 °C, 1 atm, and pure N<sub>2</sub> at 50 mL/min. As depicted in Figure 10, the excellent absorption–desorption properties of 50 wt % [DMEDA][CA] aq did not change markedly during 5 consecutive absorption–desorption cycles. The SO<sub>2</sub> absorption capacities and desorption residues were (1.76, 0.021), (1.80, 0.019), (1.78, 0.024), (1.73, 0.0260), and (1.75, 0.025) mol<sub>SO<sub>2</sub></sub>/mol<sub>IL</sub>, respectively. The results indicated that the studied absorbent exhibited satisfactory reusability. Of note, although the water content of the studied absorbent did not change obviously after 5 absorption–desorption cycles (less than 5 wt %; Table S6-2 of the Supporting Information), it is necessary to recover water by condensation reflux or replenish water to the absorbent regularly if the absorbent is used for a long time under industrial operating conditions.

**3.2.7. Desulfurization Performance.** The time-dependent SO<sub>2</sub> removal efficiency (*RE*) curves in about 2 g of 50 wt % [DMEDA][CA] aq were determined. As shown in Figure 11, the curves (40 °C) were approximately horizontal at the initial period and *RE* values were higher than 99% (0–25 min), 98%

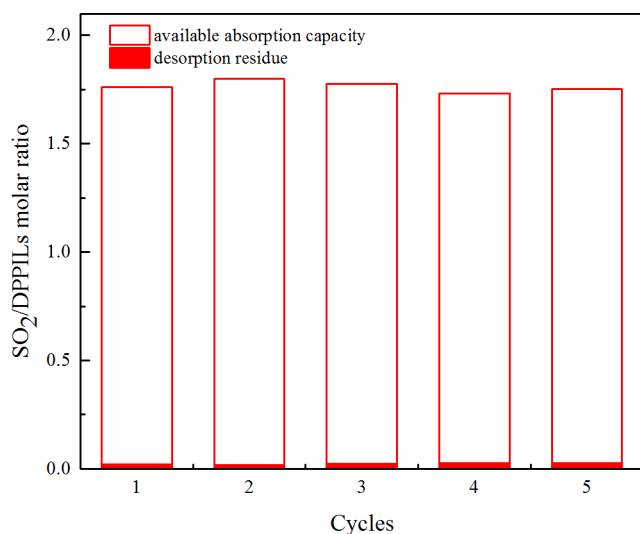


Figure 10. Reusability of 50 wt % [DMEDA][CA] aq.

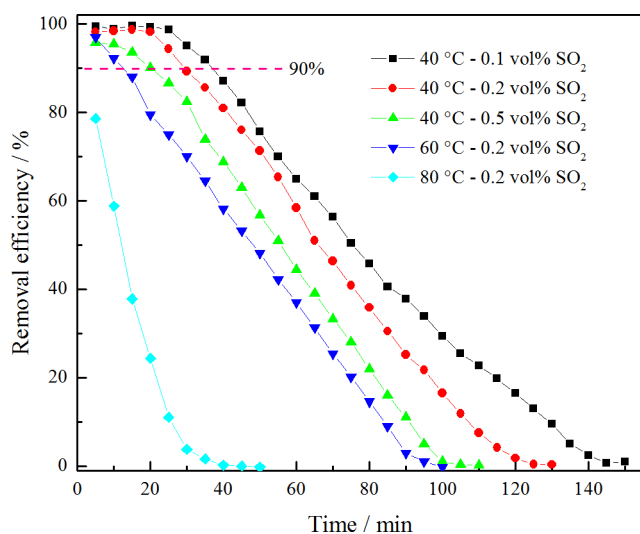


Figure 11. Desulfurization performance of 50 wt % [DMEDA][SUC] aq.

(0–20 min), and 95% (0–10 min) for the inlet  $\text{SO}_2$  concentration of 0.1, 0.2, and 0.5 vol %, respectively, indicating that inlet  $\text{SO}_2$  could be efficiently captured at 40 °C. Additionally, it could be found that the high temperature was not conducive to  $\text{SO}_2$  removal. Concretely, for the simulated flue gas with 0.2 vol %  $\text{SO}_2$ , RE of 50 wt % [DMEDA][CA] aq decreased rapidly in the absorption process at 60 and 80 °C. Nevertheless, considering that industrial desulfurization was usually carried out at 40–60 °C (amine methods) and RE of the studied absorbent was higher than 90% at the initial absorption period for the simulated flue gas with 0.1–0.5 vol %  $\text{SO}_2$  at 40–60 °C, the studied absorbent could be used as a promising substitute for the traditional amine absorbents. Meanwhile, it was noteworthy that the  $\text{SO}_2$  concentration in flue gas was usually within 0.2 vol %, whereas the excellent desulfurization performance could be obtained even if the simulated flue gas was simply bubbled through the studied absorbent within this range. Therefore, in practical application, RE of the studied absorbent could be further improved by adjusting the number of column plates and the

gas–liquid ratio to meet the stricter flue gas emission standards.

#### 4. CONCLUSION

In summary, a novel series of DPPILs were synthesized and blended with water for efficient and reversible  $\text{SO}_2$  absorption. All of the prepared absorbents presented low densities and viscosities, which were conducive to mass transfer. Effects of the DPPIL structure, DPPIL concentration, absorption temperature, and  $\text{SO}_2$  concentration on the  $\text{SO}_2$  absorption performance were comprehensively studied. It was found that all DPPILs aq could efficiently capture low-concentration  $\text{SO}_2$ . Among them, DPPILs aq based on CA showed the highest  $\text{SO}_2$  desorption efficiencies, and the available  $\text{SO}_2$  loading capacity could reach up to  $0.51 \text{ mol}_{\text{SO}_2}/\text{mol}_{\text{ILs}}$  ( $0.058 \text{ g}_{\text{SO}_2}/\text{g}_{\text{abs}}$ ) in 50 wt % [DMEDA][CA] aq at 20 °C and 0.2 vol %  $\text{SO}_2$ . The high DPPIL concentration, low absorption temperature, and high  $\text{SO}_2$  concentration were beneficial for  $\text{SO}_2$  capture. Moreover, 50 wt % [DMEDA][CA] aq also exhibited high  $\text{SO}_2/\text{CO}_2$  selectivity and excellent reusability and stability. Importantly, the  $\text{SO}_2$  removal efficiency of the studied absorbent could be higher than 98% at 40 °C for simulated flue gas with a  $\text{SO}_2$  concentration within 0.2 vol %, even by a simple bubbling method. The spectroscopic investigation suggested that the protonation of [DMEDA]<sup>+</sup> and [CA]<sup>-</sup> promoted the  $\text{SO}_2$  absorption. Comprehensively considering the simple synthesis process, low viscosity, excellent  $\text{SO}_2$  absorption–desorption properties, and superior stability, we believed that the prepared absorbents have great potential to be applied in the practical FGD process.

#### ■ ASSOCIATED CONTENT

##### Supporting Information

The Supporting Information is available free of charge on the ACS Publications website at DOI: 10.1021/acs.energyfuels.9b01745.

Characterization results, actual quantities of starting materials (Table S1), water contents of neat DPPILs (Table S2), pH values (Table S3), water loss ratios (Table S4), actual  $\text{SO}_2$  concentration (Table S5), water contents of the studied absorbents during absorption–desorption (Table S6), gravimetric  $\text{SO}_2$  absorption capacities (Table S7),  $\text{p}K_a$  values (Table S8),  $^1\text{H}$  NMR spectra of 50 wt % [DMEDA][CA] aq before and after  $\text{SO}_2$  absorption (Figure S1), and time-dependent absorption–desorption curves of  $\text{SO}_2$  in 50 wt % DPPILs aq (Figures S2 and S3) (PDF)

#### ■ AUTHOR INFORMATION

##### Corresponding Author

\*E-mail: tantaixw@tju.edu.cn.

##### ORCID

Na Yang: 0000-0003-4888-5971

Luhong Zhang: 0000-0002-7073-4793

Xiaowei Tantai: 0000-0003-2925-0444

##### Author Contributions

<sup>†</sup>Haiming Zhang and Na Yang contributed equally to this work.

##### Notes

The authors declare no competing financial interest.

## ACKNOWLEDGMENTS

The authors are grateful for the financial support from the National Key R&D Program of China (2016YFC0400406).

## REFERENCES

- (1) Spengler, J. D.; Ferris, B. G., Jr; Dockery, D. W.; Speizer, F. E. Sulfur dioxide and nitrogen dioxide levels inside and outside homes and the implications on health effects research. *Environ. Sci. Technol.* **1979**, *13* (10), 1276–1280.
- (2) Gutiérrez Ortiz, F.; Vidal, F.; Ollero, P.; Salvador, L.; Cortés, V.; Gimenez, A. Pilot-plant technical assessment of wet flue gas desulfurization using limestone. *Ind. Eng. Chem. Res.* **2006**, *45* (4), 1466–1477.
- (3) Raghunath, C. V.; Mondal, M. K. Experimental scale multi component absorption of SO<sub>2</sub> and NO by NH<sub>3</sub>/NaClO scrubbing. *Chem. Eng. J.* **2017**, *314*, 537–547.
- (4) Huang, K.; Chen, Y.-L.; Zhang, X.-M.; Xia, S.; Wu, Y.-T.; Hu, X.-B. SO<sub>2</sub> absorption in acid salt ionic liquids/sulfolane binary mixtures: Experimental study and thermodynamic analysis. *Chem. Eng. J.* **2014**, *237*, 478–486.
- (5) Karadas, F.; Atilhan, M.; Aparicio, S. Review on the use of ionic liquids (ILs) as alternative fluids for CO<sub>2</sub> capture and natural gas sweetening. *Energy Fuels* **2010**, *24* (11), 5817–5828.
- (6) Ren, S.; Hou, Y.; Tian, S.; Chen, X.; Wu, W. What are functional ionic liquids for the absorption of acidic gases? *J. Phys. Chem. B* **2013**, *117* (8), 2482–2486.
- (7) Huang, K.; Zhang, J.-Y.; Hu, X.-B.; Wu, Y.-T. Absorption of H<sub>2</sub>S and CO<sub>2</sub> in aqueous solutions of tertiary-amine functionalized protic ionic liquids. *Energy Fuels* **2017**, *31* (12), 14060–14069.
- (8) Huang, K.; Cai, D. N.; Chen, Y. L.; Wu, Y. T.; Hu, X. B.; Zhang, Z. B. Thermodynamic validation of 1-alkyl-3-methylimidazolium carboxylates as task-specific ionic liquids for H<sub>2</sub>S absorption. *AIChE J.* **2013**, *59* (6), 2227–2235.
- (9) Cui, G.; Zhang, F.; Zhou, X.; Huang, Y.; Xuan, X.; Wang, J. Acylamido-based anion-functionalized ionic liquids for efficient SO<sub>2</sub> capture through multiple-site interactions. *ACS Sustainable Chem. Eng.* **2015**, *3* (9), 2264–2270.
- (10) Wu, W.; Han, B.; Gao, H.; Liu, Z.; Jiang, T.; Huang, J. Desulfurization of flue gas: SO<sub>2</sub> absorption by an ionic liquid. *Angew. Chem., Int. Ed.* **2004**, *43* (18), 2415–2417.
- (11) Ren, S.; Hou, Y.; Wu, W.; Liu, Q.; Xiao, Y.; Chen, X. Properties of ionic liquids absorbing SO<sub>2</sub> and the mechanism of the absorption. *J. Phys. Chem. B* **2010**, *114* (6), 2175–2179.
- (12) Shang, Y.; Li, H.; Zhang, S.; Xu, H.; Wang, Z.; Zhang, L.; Zhang, J. Guanidinium-based ionic liquids for sulfur dioxide sorption. *Chem. Eng. J.* **2011**, *175*, 324–329.
- (13) Cui, G.; Wang, C.; Zheng, J.; Guo, Y.; Luo, X.; Li, H. Highly efficient SO<sub>2</sub> capture by dual functionalized ionic liquids through a combination of chemical and physical absorption. *Chem. Commun.* **2012**, *48* (20), 2633–2635.
- (14) Shiflett, M. B.; Yokozeki, A. Chemical absorption of sulfur dioxide in room-temperature ionic liquids. *Ind. Eng. Chem. Res.* **2010**, *49* (3), 1370–1377.
- (15) Wang, C.; Cui, G.; Luo, X.; Xu, Y.; Li, H.; Dai, S. Highly efficient and reversible SO<sub>2</sub> capture by tunable azole-based ionic liquids through multiple-site chemical absorption. *J. Am. Chem. Soc.* **2011**, *133* (31), 11916–11919.
- (16) Ren, S.; Hou, Y.; Tian, S.; Wu, W.; Liu, W. Deactivation and regeneration of an ionic liquid during desulfurization of simulated flue gas. *Ind. Eng. Chem. Res.* **2012**, *51* (8), 3425–3429.
- (17) Yuan, X. L.; Zhang, S. J.; Lu, X. M. Hydroxyl ammonium ionic liquids: Synthesis, properties, and solubility of SO<sub>2</sub>. *J. Chem. Eng. Data* **2007**, *52* (2), 596–599.
- (18) Wang, J.; Zeng, S.; Bai, L.; Gao, H.; Zhang, X.; Zhang, S. Novel ether-functionalized pyridinium chloride ionic liquids for efficient SO<sub>2</sub> capture. *Ind. Eng. Chem. Res.* **2014**, *53* (43), 16832–16839.
- (19) Zhang, L.; Zhang, Z.; Sun, Y.; Jiang, B.; Li, X.; Ge, X.; Wang, J. Ether-functionalized ionic liquids with low viscosity for efficient SO<sub>2</sub> capture. *Ind. Eng. Chem. Res.* **2013**, *52* (46), 16335–16340.
- (20) Huang, K.; Lu, J.-F.; Wu, Y.-T.; Hu, X.-B.; Zhang, Z.-B. Absorption of SO<sub>2</sub> in aqueous solutions of mixed hydroxylammonium dicarboxylate ionic liquids. *Chem. Eng. J.* **2013**, *215*, 36–44.
- (21) Qian, J.; Ren, S.; Tian, S.; Hou, Y.; Wang, C.; Wu, W. Highly efficient and reversible absorption of SO<sub>2</sub> by aqueous triethylenetetramine tetralactate solutions. *Ind. Eng. Chem. Res.* **2014**, *53* (39), 15207–15212.
- (22) Sun, Y.; Zhang, Y.; Zhang, L.; Jiang, B.; Gu, W.; Yang, H. SO<sub>2</sub> capture using pH-buffered aqueous solutions of protic triamine-based ionic liquid. *Energy Fuels* **2017**, *31* (4), 4193–4201.
- (23) Yoshizawa, M.; Xu, W.; Angell, C. A. Ionic liquids by proton transfer: Vapor pressure, conductivity, and the relevance of ΔpKa from aqueous solutions. *J. Am. Chem. Soc.* **2003**, *125* (50), 15411–15419.
- (24) Belieres, J.-P.; Angell, C. A. Protic ionic liquids: Preparation, characterization, and proton free energy level representation. *J. Phys. Chem. B* **2007**, *111* (18), 4926–4937.
- (25) Rahmani, F.; Mowla, D.; Karimi, G.; Golkhar, A.; Rahmatmand, B. SO<sub>2</sub> removal from simulated flue gas using various aqueous solutions: Absorption equilibria and operational data in a packed column. *Sep. Purif. Technol.* **2015**, *153*, 162–169.
- (26) Tang, Z.-g.; Zhou, C.-c.; Chen, C. Studies on flue gas desulfurization by chemical absorption using an ethylenediamine-phosphoric acid solution. *Ind. Eng. Chem. Res.* **2004**, *43* (21), 6714–6722.
- (27) Lim, S. R.; Hwang, J.; Kim, C. S.; Park, H. S.; Cheong, M.; Kim, H. S.; Lee, H. Absorption and desorption of SO<sub>2</sub> in aqueous solutions of diamine-based molten salts. *J. Hazard. Mater.* **2015**, *289*, 63–71.
- (28) Zhang, K.; Ren, S.; Meng, L.; Hou, Y.; Wu, W.; Bao, Y. Efficient and reversible absorption of sulfur dioxide of flue gas by environmentally benign and stable quaternary ammonium inner salts in aqueous solutions. *Energy Fuels* **2017**, *31* (2), 1786–1792.
- (29) Zhang, K.; Ren, S.; Hou, Y.; Wu, W.; Bao, Y. Sodium lactate aqueous solution, a green and stable absorbent for desulfurization of flue gas. *Ind. Eng. Chem. Res.* **2017**, *56* (46), 13844–13849.
- (30) Zhao, T.; Zhang, X.; Tu, Z.; Wu, Y.; Hu, X. Low-viscosity diamino protic ionic liquids with fluorine-substituted phenolic anions for improving CO<sub>2</sub> reversible capture. *J. Mol. Liq.* **2018**, *268*, 617–624.
- (31) Oncsik, T.; Vijayaraghavan, R.; MacFarlane, D. R. High CO<sub>2</sub> absorption by diamino protic ionic liquids using azolide anions. *Chem. Commun.* **2018**, *54* (17), 2106–2109.
- (32) Vijayaraghavan, R.; Pas, S. J.; Izgorodina, E. I.; MacFarlane, D. R. Diamino protic ionic liquids for CO<sub>2</sub> capture. *Phys. Chem. Chem. Phys.* **2013**, *15* (46), 19994–19999.
- (33) Mumford, K. A.; Pas, S. J.; Linseisen, T.; Statham, T. M.; Nicholas, N. J.; Lee, A.; Kezia, K.; Vijayaraghavan, R.; MacFarlane, D. R.; Stevens, G. W. Evaluation of the protic ionic liquid, *N,N*-dimethylaminoethylammonium formate for CO<sub>2</sub> capture. *Int. J. Greenhouse Gas Control* **2015**, *32*, 129–134.
- (34) Simons, T. J.; Verheyen, T.; Izgorodina, E. I.; Vijayaraghavan, R.; Young, S.; Pearson, A. K.; Pas, S. J.; MacFarlane, D. R. Mechanisms of low temperature capture and regeneration of CO<sub>2</sub> using diamino protic ionic liquids. *Phys. Chem. Chem. Phys.* **2016**, *18* (2), 1140–1149.
- (35) Vijayaraghavan, R.; Oncsik, T.; Mitschke, B.; MacFarlane, D. Base-rich diamino protic ionic liquid mixtures for enhanced CO<sub>2</sub> capture. *Sep. Purif. Technol.* **2018**, *196*, 27–31.
- (36) Meng, X.; Wang, J.; Xie, P.; Jiang, H.; Hu, Y.; Chang, T. Structure and SO<sub>2</sub> absorption properties of guanidinium-based dicarboxylic acid ionic liquids. *Energy Fuels* **2018**, *32* (2), 1956–1962.
- (37) Meng, X.; Wang, J.; Jiang, H.; Zhang, X.; Liu, S.; Hu, Y. Guanidinium-based dicarboxylic acid ionic liquids for SO<sub>2</sub> capture. *J. Chem. Technol. Biotechnol.* **2017**, *92* (4), 767–774.
- (38) Wu, Z.; Hou, Y.; Wu, W.; Ren, S.; Zhang, K. Efficient removal of sulfuric acid from sodium lactate aqueous solution based on



common-ion effect for the absorption of SO<sub>2</sub> of flue gas. *Energy Fuels* **2019**, *33* (5), 4395–4400.

(39) Tian, S.; Hou, Y.; Wu, W.; Ren, S.; Wang, C.; Qian, J. Reversible absorption of SO<sub>2</sub> from simulated flue gas by aqueous calcium lactate solution. *J. Taiwan Inst. Chem. Eng.* **2015**, *54*, 71–75.

(40) Li, Q.; Weng, S.; Wu, J.; Zhou, N. Comparative study on structure of solubilized water in reversed micelles. 1. FT-IR spectroscopic evidence of water/AOT/n-heptane and water/Na-DEHP/n-heptane systems. *J. Phys. Chem. B* **1998**, *102* (17), 3168–3174.

(41) Ogino, J.; Moore, R. E.; Patterson, G. M.; Smith, C. D. Dendroamides, new cyclic hexapeptides from a blue-green alga. Multidrug-resistance reversing activity of dendroamide A. *J. Nat. Prod.* **1996**, *59* (6), 581–586.

(42) Qiao, X.; Zhang, F.; Sha, F.; Shi, H.; Zhang, J. Solubility properties and absorption mechanism investigation of dilute SO<sub>2</sub> in propylene glycol monomethyl ether+dimethyl sulfoxide system. *J. Chem. Eng. Data* **2017**, *62* (6), 1756–1766.

(43) Luo, Q.; Feng, B.; Liu, Z.; Zhou, Q.; Zhang, Y.; Li, N. Experimental study on simultaneous absorption and desorption of CO<sub>2</sub>, SO<sub>2</sub>, and NO<sub>x</sub> using aqueous N-methyldiethanolamine and dimethyl sulfoxide solutions. *Energy Fuels* **2018**, *32* (3), 3647–3659.

(44) Sun, Z.; Zhao, Y.; Gao, H.; Hu, G. Removal of SO<sub>2</sub> from flue gas by sodium humate solution. *Energy Fuels* **2010**, *24* (2), 1013–1019.

(45) Hong, S. Y.; Kim, H.; Kim, Y. J.; Jeong, J.; Cheong, M.; Lee, H.; Kim, H. S.; Lee, J. S. Nitrile-functionalized tertiary amines as highly efficient and reversible SO<sub>2</sub> absorbents. *J. Hazard. Mater.* **2014**, *264*, 136–143.

(46) Heldebrant, D. J.; Koech, P. K.; Yonker, C. R. A reversible zwitterionic SO<sub>2</sub>-binding organic liquid. *Energy Environ. Sci.* **2010**, *3* (1), 111–113.

(47) Chen, K.; Lin, W.; Yu, X.; Luo, X.; Ding, F.; He, X.; Li, H.; Wang, C. Designing of anion-functionalized ionic liquids for efficient capture of SO<sub>2</sub> from flue gas. *AIChE J.* **2015**, *61* (6), 2028–2034.

(48) Cui, G.; Zhao, N.; Li, Y.; Wang, H.; Zhao, Y.; Li, Z.; Wang, J. Limited number of active sites strategy for improving SO<sub>2</sub> capture by ionic liquids with fluorinated acetylacetonate anion. *ACS Sustainable Chem. Eng.* **2017**, *5* (9), 7985–7992.

(49) Jiang, B.; Zhang, H.; Zhang, L.; Zhang, N.; Huang, Z.; Chen, Y.; Sun, Y.; Tantai, X. Novel deep eutectic solvents for highly efficient and reversible absorption of SO<sub>2</sub> by preorganization strategy. *ACS Sustainable Chem. Eng.* **2019**, *7* (9), 8347–8357.